Characterization of Subsurface Flow Dynamics for Forecasting of Solar Activity

Alexander Kosovichev[1,2], Viacheslav Sadykov[2,3]

[1]New Jersey Institute of Technology, [2]NASA Ames Research Center (U.S.A.), [3]Bay Area Environmental Research Institute

Evolution of large-scale magnetic field structures in the solar photosphere and corona is controlled by motions beneath the visible surface of the Sun. Subsurface plasma flows play a critical role in formation and evolution of active regions and their activity. We analyze subsurface flow maps provided by the local helioseismology pipeline from the Helioseismic and Magnetic Imager (HMI) data on board the Solar Dynamics Observatory, and investigate links between flow characteristics and magnetic activity. The primary goal is to determine flow descriptors, which can improve solar activity forecasts. In particular, by employing machine learning classifiers, we test how the flow helicity and velocity shear descriptors can improve the prediction of initiation of flares and CME eruptions.

Motivation

- The primary goal of our study is to improve characterization and physical understanding and enhance the prediction of solar transient events by utilizing data and physical descriptors from Magnetogram and Subsurface Flow Maps obtained by local helioseismology.
- The processes, by which the magnetic energy is stored, entering, and leaving of solar active regions, are critically linked to the flow patterns in active regions. Large-scale organized flows are developed spontaneously in subsurface layers due magnetic flux emergence and its interaction with the existing magnetic field of active regions. This process forms stressed magnetic configurations that trigger solar eruptions.

Measurements of Subsurface Flows by Time-Distance Helioseismology

- The computational pipeline for studying the subsurface dynamics of active regions takes the Carrington coordinates of active regions from the Solar Region Summary (SRS) database, compiled by the NOAA Space Weather Prediction Center (SWPC), and uses these coordinates as the central points of -degree areas tracked for 10 days during their passage on the solar disk.
- This setup allows us to follow the evolution of active region areas even before the magnetic flux emergence and after the decay. The 3D subsurface flow maps are calculated from the tracked Dopplergrams that are remapped onto the heliographic coordinates using the Postel's projection (transverse cylindrical projection that preserves the distance along great circles).
- Each tracked, 8-hour long, datacube consists of 640 Dopplergrams of pixels with the spatial resolution of 0.06 degree/pixel, and 45-sec time cadence. The tracked datacubes are processed through the Time-Distance Helioseismology Pipeline (Zhao et al. 2012), and the output represents acoustic travel-time maps calculated with 0.12-deg sampling for the whole tracked areas (pixels).

Time-distance pipeline data flow chart

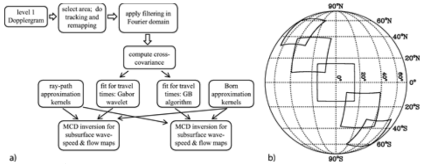

Measurements of Acoustic Travel Times

The travel-times are calculated for eleven annuli located at different distances from central points corresponding to -binned original Dopplergram pixels. The signals of acoustic waves traveling between the central points and the surrounding annuli are calculated from the HMI Doppler velocity measurements as the corresponding cross-covariance functions. The cross-covariances are computed in the Fourier space, and phase-space filters are applied to isolate the signals corresponding to each of the travel distances.

$$\psi(\tau,\Delta)=\int_0^T f(t,\boldsymbol{r})f^*(t+\tau,\boldsymbol{r}+\Delta)dt$$

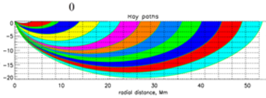

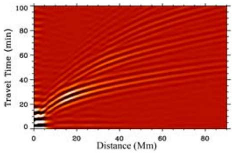

The travel times are calculated by two different methods: 1) the Gabor wavelet fitting (Kosovichev and Duvall, 1997)

$$G(A,\omega_0,\delta\omega,\tau_{\rm p},\tau_{\rm g};t)=A\cos\left\{\omega_0(t-\tau_{\rm p})\right\}\exp\left(-\frac{\delta\omega^2}{4}(t-\tau_{\rm g})^2\right)$$

and 2) a cross-correlation with a reference (Gizon & Birch 2002).

Travel Time Inversion

The travel times are used to infer the 3D maps of subsurface flows by solving an inverse problem. It is formulated as the set of linear integral equations whose kernels are calculated by using the ray-path theory and the first Born approximation.

$$\delta\tau(\boldsymbol{x}_1,\boldsymbol{x}_2)=\iiint_V \mathrm{d}\boldsymbol{r}\,\boldsymbol{K}(\boldsymbol{r};\boldsymbol{x}_1,\boldsymbol{x}_2)\cdot\boldsymbol{v}(\boldsymbol{r})$$

The travel times are used to infer the 3D maps of subsurface flows by solving an inverse problem. It is formulated as the set of linear equations for grid points (*l,j,k*) for each surface point (λ,μ) and travel distance (ν).

$$\delta\tau_l^{\lambda\mu\nu}=\sum_{ijk,l}A_{ijk,l}^{\lambda\mu\nu}\tilde{v}_l^{ijk}, \qquad \tilde{v}_l^{ijk}=[v_x^{ijk},v_y^{ijk},v_z^{ijk}]/c^k$$

The travel times are used to infer the 3D maps of subsurface flows by solving an inverse problem. It is formulated as the set of linear integral equations. Regularized solutions are determined by the Multi-Channel Deconvolution (MCD) method, and the regularization parameters are chosen to suppress noise and represent a smooth solution.

References

Kosovichev, A.G., Duvall, T.L. Jr.: 1997, *Solar Convection and Oscillations and Their Relationship*, Astrophys. Astron.Libr. **225**, Dordrecht, 241
Gizon, L., Birch, A.C.: 2002, *Astrophys. J.* **571**, 966
Zhao, J., Couvidat, S., Bogart, R.S., et al. 2012, *Solar Phys.*, **275**, 375

Subsurface Dynamics During Emergence and Evolution of Active Regions

We used the SDO/HMI time-distance helioseismology pipeline (http://jsoc.stanford.edu) to infer 3D subsurface flow maps during the emergence and evolution of Active Regions. The travel times are used for reconstruction of subsurface flows in 8 subsurface layers in the depth ranges: 0-1, 1-3, 3-5, 5-7, 7-10, 10-13, 13-17, and 17-21 Mm, and with the horizontal spatial sampling of 0.12 degrees (1.5 Mm).
The horizontal flows for AR12673 in the depth range of 1-3 Mm are shown by arrows. The background color images are the corresponding photospheric magnetograms.

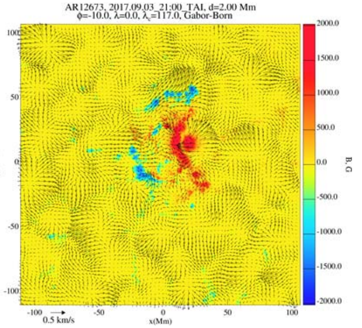

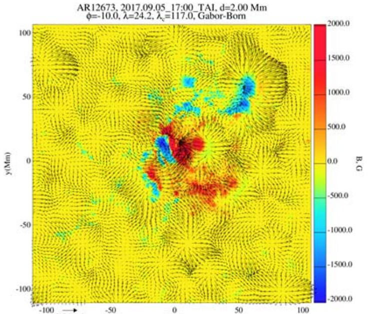

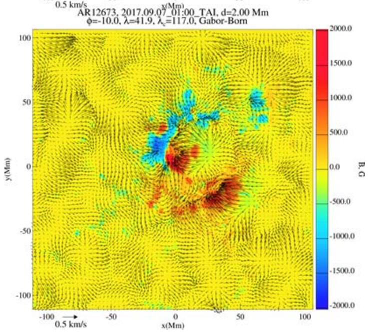

Calculation of Flow Characteristics

We derive physical descriptors to characterize the subsurface flow maps:

1) a layer-average horizontal divergence computed based on the horizontal velocity component;
2) a layer-average vertical component of the velocity curl (vorticity);
3) a proxy for the kinetic helicity defined as a products of the horizontal divergence and the vertical component of vorticity.

The usage of the horizontal component of the velocity is considered as its vertical component has significantly larger uncertainties. The subsurface layers closest to the surface (0-1 Mm, 1-3 Mm, and 3-5 Mm deep) are more relevant to the short-term active region evolution, and have less uncertainties. However, descriptors of the deeper layers can potentially result in longer lead times and improve 24-hour ahead forecasts, and are also analyzed.

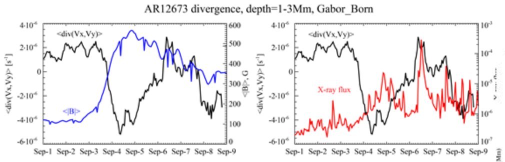

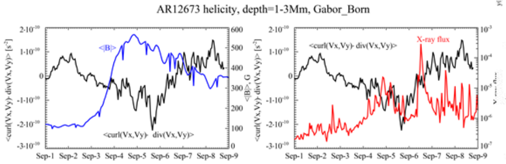

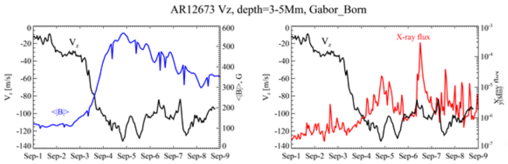

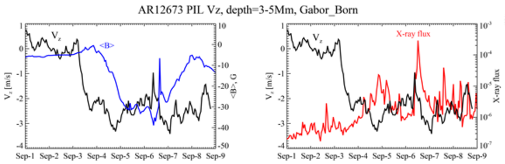

The flow maps reveal strong (v>1km/s) shearing flows beneath the active region, and, in particular, in the area of the Polarity Inversion Line (PIL), which was the source of several flares including the X9.3 flare of Sept. 6, 2017.

Left panels: Comparison of the flow characteristics (mean divergence, helicity proxy and vertical velocity component) with the mean magnetic flux (represented in the plots by mean unsigned magnetic field) shows the formation of converging downdrafts beneath the active region and an increase in kinetic helicity.

Right panels: Comparison of the flow characteristics with the soft X-ray flux (1-hour averages from GOES data) reveals a correlation of the large flares with enhancements of flow divergence. There is an evidence of upflows prior the big flares (X2.2. and X9.3 of Sept. 6, and X1.3 of Sept.7). It becomes more apparent for upflows in the PIL area (bottom panels). It seems that the upflows started prior the X-ray impulses and prior the flare photospheric impact (seen as a spike in the bottom left panel).

Correlation of Flow Characteristics with Flare Productivity

We define the flare productivity of the active region as $P = N_C + 10\times N_M + 100\times N_X$ where N_C, N_M, and N_X are the total number of C-class, M-class, and X-class GOES flares happened in the AR within 24 or 48 hours from the considered moment. The flare productivity is used for correlation analysis with the AR magnetic and flow descriptors.

We analyze correlations of the derived descriptors with the flare productivity of the parental active region within the next 24 hour window. In addition to classically-used Pearson's correlation coefficients which checks for linear dependence between the set of pairs of parameters, we plan to analyze non-parametric Kendall's tau correlation coefficient defined as:

$$\tau=\frac{2}{n(n-1)}\sum_{i<j}\operatorname{sgn}(x_i-x_j)\operatorname{sgn}(y_i-y_j),$$

where the x_i and y_i are the values of the considered pair of parameter; sgn is a sign operator; n is a number of elements in each data set. Kendall's tau ranges between -1 and 1, and its value is expected to be 0 for independent data sets.

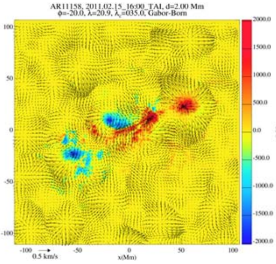

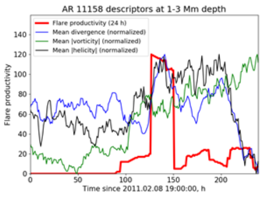

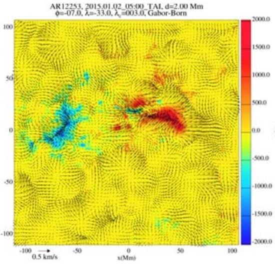

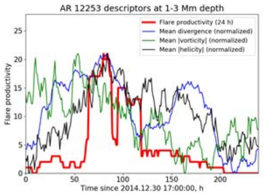

Table 1. Strongest Kendall's tau rank correlation coefficients and corresponding time lags (varying from 0 h to 24 h) found for subsurface flow map descriptors at 1-3 Mm depth and flare productivity. The correlations are obtained for 8 ARs tracked for 10 days with 1 hour cadence. Red entries indicate cases where correlation coefficients were not statistically-significant (corresponding p-value is < 0.05).

Active Region	Total divergence at 1-3 Mm	Total vorticity at 1-3 Mm	Total kinetic helicity at 1-3 Mm
11158	0.14 / 0 h	0.53 / 7 h	0.47 / 0 h
11283	0.61 / 0 h	-0.27 / 18 h	0.40 / 15 h
11305	0.65 / 20 h	-0.25 / 23 h	0.46 / 2 h
11618	0.30 / 24 h	-0.43 / 7 h	0.08 / 0 h
11875	-0.38 / 0 h	0.10 / 7 h	-0.16 / 22 h
11967	0.15 / 6 h	0.20 / 0 h	0.48 / 11 h
12253	0.41 / 24 h	0.54 / 24 h	0.65 / 2 h
12673	0.14 / 19 h	0.65 / 0 h	0.22 / 20 h

Summary

Helioseismic flow maps reveal links between subsurface flows and formation of the sheared magnetic structure with long Polarity Inversion Line (PIL) which became a source of substantial flaring activity. In particular, the helioseismic data reveal correlation of increased flow convergence with flare productivity of active regions. We plan to incorporate the flow descriptors in the machine-learning flare prediction tools.